Pediatr Surg Int (2006) 22: 84–89
DOI 10.1007/s00383-005-1589-0

ORIGINAL ARTICLE

Johannes Leonhardt · Martin Stanulla
Reinhard von Wasielewski · Julia Skokowa
Joachim Kübler · Benno M. Ure · Claus Petersen

Gene expression profile of the infective murine model for biliary atresia

Published online: 18 November 2005

Abstract One hypothesis of the pathogenesis of biliary atresia (BA) is a virus-induced and immune-mediated injury to bile duct cells as mimicked in the rotavirus-induced murine model. This theory is supported by studies showing a predominant T helper cell response type 1-like phenotype of inflammation with increased interferon gamma-induced chemokines in the liver of humans and mice suffering from BA. Recent gene expression profiling studies using microarray analysis showed the induction of a proinflammatory state in human liver specimens with high analogies in extrahepatic biliary tissue of BA mice. The aim of the present study was a microarray analysis of gene expression in the liver of Balb/c mice, comparing infected mice that show the phenotype of BA versus infected mice without symptoms, thus trying to elucidate genes that are not related to the viral origin of this model, but to the specific pathogenesis of the clinical picture of BA. Fifteen μg of RNA, each of three BA-positive and three BA-negative mice, were pooled and comparatively hybridized to spotted cDNA microarrays containing 250 key genes with high relevance to immunological settings. We identified the 40 genes most differentially expressed in mice with and without BA. The majority of genes with higher expression in BA-positive mice encoded proinflammatory cytokines involved in the Th1 pathway, such as CCL2, CCL5, CCR5, CXCL10, CCL2, IL1F5 and in apoptosis, such as DDR3 and granzyme A and B. In this initial study of the molecular characterization of our RRV-induced BA mouse model system, we also found potential novel candidates important to BA etiology, such as growth hormone receptor and insulin-like growth factor. Of particular interest, very low expression of TIMD2 was observed in BA-positive mice. TIMD2 plays a critical role in the regulation of a Th2-type response through the inhibition of IFN gamma.

J. Leonhardt (✉) · J. Kübler · B. M. Ure · C. Petersen
Department of Pediatric Surgery, Hannover Medical School,
Carl-Neuberg-Str. 1, 30625 Hannover, Germany
E-mail: leonhardt.johannes@mh-hannover.de
Tel.: +49-511-5329260
Fax: +49-511-5329059

M. Stanulla · J. Skokowa
Department of Pediatric Hematology and Oncology,
Hannover Medical School, Carl-Neuberg-Str. 1,
30625 Hannover, Germany

R. von Wasielewski
Department of Pathology, Hannover Medical School,
Carl-Neuberg-Str. 1, 30625 Hannover, Germany

Introduction

Biliary atresia (BA) is a rare hepatobiliary disorder in newborns with poor prognosis [1]. A progressive, inflammatory process leads to complete obstruction of bile ducts resulting in biliary cirrhosis. The precise etiopathogenesis of BA is not understood, but several studies support the hypothesis that BA is a virus-induced, immune-mediated disease in a genetically susceptible condition [2]. Recent investigations revealed that BA is associated with T helper cell response type 1-mediated portal tract inflammation and important roles for interleukin (IL)-2, interferon (IFN) gamma, IL-12, tumor necrosis factor α (TNF α) and macrophage activation have been suggested [3].

For detailed examination, different research groups used the unique BA animal model, in which the infection of newborn mice with Rhesus Rotavirus (RRV) leads to atresia of extrahepatic bile ducts in approximately 80% of the animals (s. Fig. 1a, b, c) [4–7]. In this model, the absence of IFN gamma completely prevented the obliteration of bile ducts, which resulted in the resolution of symptoms verifying the critical role of this cytokine in the inflammatory process [8]. This group also used genome-wide microarray expression analysis of liver biopsies from patients with BA and approved up-regulation of many pro-inflammatory genes and down-regulation of immunoglobuline genes, suggesting the

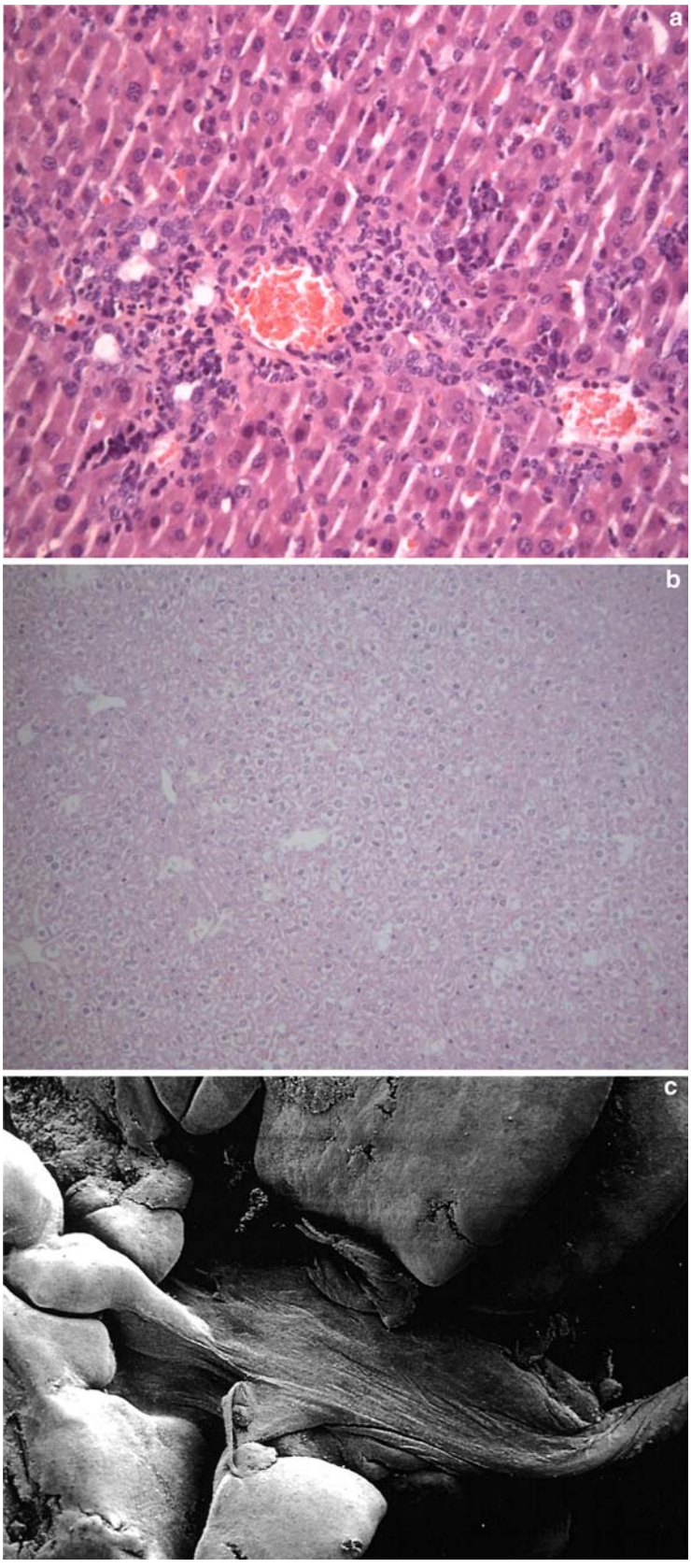

Fig. 1 **a** Hematoxylin eosin (HE) staining (25× magnification) of a 10 day old mouse after RRV infection with periductal inflammation in the liver. **b** HE staining (16× magnification) of a 10 day old mouse after RRV infection without signs of biliary atresia **c** Electron microscope shows a long-distance atresia of the extrahepatic murine bile duct

inhibition of Th-2 cytokines [9]. Sequential expression of IFN gamma-inducers in the biliary tract of BA mice points towards an activated network that triggers expression of other genes leading to progression of bile duct inflammation leading to complete obstruction [10]. Our study group demonstrated that the inactivation of

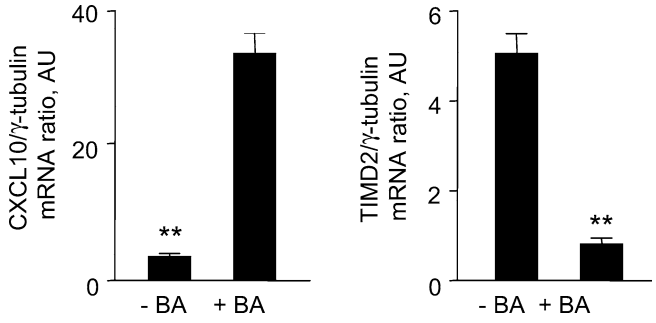

Fig. 2 mRNA expression of CXCL-10 in BA-positive mouse (+BA) and TIMD2 in BA-negative mouse (-BA) in relation to the housekeeping gene gamma-Tubulin. AU (arbitrary unit)

type I IFN receptors significantly increases the incidence of BA in mice. This was independent of the presence of type II IFN receptors. Type I IFN-linked deregulation of the innate immune system appears to be crucial for the induction of biliary atresia in mice [unpublished data]. The aim of the present study was to demonstrate differences between Balb/c mice, with and without BA, after RRV infection by generating liver gene expression profiles using cDNA microarrays, thus trying to elucidate genes that are not related to the viral origin, but to the specific pathogenesis of BA and to issue a candidate gene list of BA in this model system for comparison with previous reports.

Materials and methods

Virus

The strain of RRV used was kindly provided by Marie Riepenhoff-Talty and titered as described previously [6]. Briefly, organs were ultrasonically homogenized and centrifuged at 4°C and 4,000 rpm in a 3,350 rotor in a Heraeus Minifuge GL (Heraeus, Hanau, Germany). Titration of the virus in graded, logarithmic dilutions was performed in tissue culture microtiter plates with confluent cells. Readings of the titers were carried out after 4 days of incubation under standard cell culture conditions and expressed as plaque forming units (pfu/ml).

Animals

Balb/c mice were kept pathogen-free in laminar-flow cages and housed in a room with a 12 h dark–light cycle. Newborn mice were intraperitoneally infected with 20 µl of 1×10^6 pfu of RRV within 24 h post partum. Animals were checked daily for icterus of the non fur-covered skin, acholic stools and bilirubinuria. All procedures were in compliance with the national regulations for protection of animals, under supervision of the appropriate veterinarian (permit no. 03/693 from the Bezirksregierung, Hannover, Germany).

Dissection and histology

All mice were killed 10 days after infection and prepared under a dissecting microscope. The liver, extrahepatic bile duct and the brain (for virus titration) were harvested for histological examination (fixation, paraffin embedding, microsection and hematoxilin and eosin (H.E.) staining) and RNA isolation.

RNA extraction

Total RNA of the primary set was isolated with Trizol reagent (Invitrogen, Paisley, UK) and subsequently passed over a Qiagen RNeasy column (Qiagen, Hilden, Germany) for the removal of small fragments. Total RNA was quantified and validated for integrity using the Bioanalyzer 2100 (Agilent, Palo Alto, CA, USA).

Microarray and data analysis

Spotted murine cDNA microarrays composed of 250 key genes with high relevance in immunological in vitro and in vivo settings were used (Miltenyi, PIQOR™ Cytokines & Receptors, Cologne, Germany). Each PIQOR™ microarray contains six housekeeping genes and six controls (herring sperm DNA, salt, four artificial control RNAs) for the correct quantification of the differential expression. Genes are spotted in quadruplicates. Fifteen µg RNA, each of three BA-positive and three BA-negative mice, were pooled, the two pools labeled with different fluorescent dyes (Cy5-deoxyuridine triphosphate [dUTP] and Cy3-dUTP) and comparatively hybridized to an array as previously described [11]. Briefly, for each spot, the local signal was measured inside a fixed circle of 350 µm diameter and the background was measured outside the circle within specified rings 40 µm distant to the signal and 40 µm wide. Signal and background were taken to be the average of pixels between defined low and high percentages of maximum intensity, with percentage parameter settings for low/high being 0/97% for signal and 0/80% for background. Local background was subtracted from the signal to obtain the net signal intensity and the ratio of Cy5/Cy3. The ratios were normalized to the median of all ratios by using only those spots for which the fluorescent intensity in one of the two channels was thrice the negative control. Subsequently, the mean of the ratios of four corresponding spots representing the same cDNA were computed. The negative control for each array was computed as the mean of the signal intensity of two spots representing herring sperm and two spots representing spotting buffer, only. Only genes displaying a net signal intensity threefold higher in the sample than in the negative control were used for further analysis. Also, coefficients of variation of the ratios of four corresponding spots representing the same cDNA were computed. Coefficients of variation of 30% and less were considered acceptable.

Table 1 Virus load of infected mice without differences in the virus-titer between mice with and without BA

Balb/C mice no.	Days post infection	BA	Virus load (pfu) liver/brain
1	10	yes	$1\times10^4/10^3$
2	10	yes	$1\times10^6/10^5$
3	10	yes	$1\times10^2/10^3$
4	10	no	$1\times10^8/10^6$
5	10	no	$1\times10^3/10^4$
6	10	no	$1\times10^6/10^6$

Quantitative RT-PCR

To validate the array results, we performed quantitative RT-PCR on selected genes using the individual samples contributing to the RNA pools. We used random hexamer priming and MuLV reverse transcriptase (Fermentas, Hannover, MD) to generate cDNA. PCR was carried out on a 7300 Real-Time PCR System (Applied Biosystems, Darmstadt, Germany) using the QuantiTect SYBR Green PCR kit (Qiagen) as described in the manufacturer's instructions. Primer pairs for TIMD2, CXCL10 and gamma-Tubulin were chosen from Qiagen's Quantitect Primer Assay list. Reactions were carried out as previously described [12] under the following conditions: 95°C for 15 min, then 40 cycles of 94°C for 15 s, 55°C for 30 s and 72°C for 30 s. Melting curves analyses were performed to verify the amplification specificity. For quantification, gene expression of the target sequence was normalized in relation to the expressed housekeeping gene gamma-Tubulin (s. Fig. 2).

Results

From one litter, we sacrificed three animals with the typical clinical and histomorphological signs of biliary

Table 2 Top 40 differentially regulated genes comparatively hybridizing biliary atresia-positive and negative mice after infection with rhesus rotavirus

Gene name	UniGene annotation	Fold-change/Coefficient of variation
TIMD2: T-cell immunoglobulin and mucin domain containing 2	Mm.234654	0.16/18%
TNFRSF19L: tumor necrosis factor receptor superfamily, member 19-like	Mm.40336	0.22/11%
GHR: growth hormone receptor	Mm.3986	0.22/21%
CXCL7: chemokine (C-X-C motif) ligand 7	Mm.293614	0.28/29%
CCL19: chemokine (C-C motif) ligand 19	Mm.258946	0.29/13%
IGF1: insulin-like growth factor I	Mm.268521	0.30/10%
TBLYM: transcription factor TBLYM	Mm.94519	0.34/26%
OSM: oncostatin M precursor	Mm.131422	0.43/5%
SCYE1: small inducible cytokine subfamily E member 1	Mm.235137	0.44/11%
IL1RN: interleukin-1 receptor antagonist	Mm.882	0.46/21%
SOCS6: suppressor of cytokine signaling 6	Mm.91920	0.46/24%
IL17BR:interleukin-17B receptor	Mm.269363	0.47/16%
IGF2: insulin-like growth factor II	Mm.3862	0.50/8%
IL13: interleukin-13	Mm.1284	0.53/4%
GPR44: putative G protein-coupled receptor GPR44	Mm.56903	0.55/27%
TNFRSF19: tumor necrosis factor receptor superfamily member 19	Mm.281356	0.58/9%
CSF1: macrophage colony stimulating factor-1	Mm.795	0.59/21%
CXCL12: chemokine (C-X-C motif) ligand 12	Mm.303231	0.60/11%
TNFRSF9: tumor necrosis factor receptor superfamily member 9	Mm.244187	0.61/27%
CCR4: chemokine (C-C motif) receptor 4	Mm.1337	0.63/21%
TNFRSF5: tumor necrosis factor receptor superfamily 5	Mm.271833	1.57/22%
CXCL9: chemokine ligand 9	Mm.766	1.68/21%
TNFRSF11B: tumor necrosis factor receptor superfamily 11B	Mm.15383	1.61/13%
GZMA: GRANZYME A	Mm.15510	1.65/19%
IFRD1: interferon-related developmental regulator 1	Mm.168	1.71/16%
DDR3: death domain receptor 3	Mm.101198	1.71/30%
EDA: ECTODYSPLASIN A.	Mm.328086	1.77/17%
CCL2: chemokine (C-C motif) ligand 2	Mm.290320	1.91/17%
IL22R: IL-22 receptor, alpha 1	Mm.261647	1.91/30%
CXCL16: chemokine (C-X-C motif) ligand 16	Mm.46424	1.93/18%
CCR5: chemokine (C-C motif) receptor 5	Mm.14302	2.00/30%
PRF1: PERFORIN 1	Mm.240313	2.06/16%
TXLN: TAXILIN	Mm.268863	2.14/30%
F3: coagulation factor III	Mm.273188	2.51/9%
IL23R: interleukin-23 receptor	Mm.221227	2.59/17%
MPL: thrombopoietin receptor	Mm.4864	2.66/11%
IL1F5: interleukin 1 family member 5	Mm.29261	2.91/4%
GZMB: GRANZYME B	Mm.14874	3.49/28%
CCL5: chemokine (C-C motif) ligand 5	Mm.284248	6.06/29%
CXCL10: chemokine (C-X-C motif) ligand 10	Mm.877	6.72/5%

atresia and three mice without jaundice 10 days after RRV infection. Under the dissection microscope extrahepatic bile ducts demonstrated different varieties of biliary atresia in the three BA mice, as previously demonstrated by electron microscopic examination (s. Fig. 1c) [13]. After H.E. staining, inflammation of liver parenchyma and proliferation of intrahepatic bile ducts in three mice with BA and only moderate inflammation of the liver and the extrahepatic biliary tract in the other three was shown (s. Fig. 1a,b). Similar to earlier observations, virus titers were not significantly different between the two groups (s. Table 1) [6, 14].

Using microarrays containing cytokines and receptors with high relevance to immunological settings, we identified the 40 genes most differentially expressed in the liver of mice with and without BA (s. Table 2). Functional classification of the genes was performed using information available in PubMed and Unigene (http://www.ncbi.nlm.nih.gov/Unigene). The majority of genes with higher expression in BA-positive mice encoded (1) proinflammatory cytokines involved in the Th1-cell pathway, activation of macrophages and autoimmune inflammation in accordance to the findings of Bezerra: IL1-F5, IL-22 receptor, IL-23 receptor, the IFN gamma-induced chemokine CXCL10 and the complement component perforin 1 (C9), an effector of humoral immunity participating in the enhancement of T-cell response [15] and (2) cytokines, that trigger apoptosis, such as granzyme A and B and DDR3 via stimulation of NF kappa beta activation. Furthermore, we found the chemokine CCR5 and its ligand CCL5 and CCL2. The latter two beeing chemoattractive for monocytes and Th-1 cells promoting the recruitment of T-cells to the liver [16].

The genes with lower expression in BA-positive mice encoded genes involved in (1) immune response, such as TBLYM (T-box 21), a Th1-cell-specific transcription factor, that controls the expression of IFN gamma, TNFRSF19L, a member of the TNF receptor superfamily, as well as CCL19, the macrophage inflammatory ligand protein activating CD8+ T-cells and (2) novel candidate genes, such as insulin-like growth factor 1 (IGF-1), the growth hormone receptor (GHR) and TIMD2. The TIM gene family encodes cell surface receptors that are involved in the regulation of Th1- and Th2-cell-mediated immunity. TIMD2 is up-regulated in Th2 cells and down-regulated in Th1 cells, playing a critical role in the regulation of a Th2-type response with inhibition of IFN gamma [17].

Discussion

The precise role of the immune system in the pathogenesis of biliary atresia is not understood. However, investigations in histological sections of patients, as well as experimental studies using the BA mice model, have demonstrated an inflammatory process around the biliary tree that appears to contribute to the process of BA [3,6,14]. Studies to further identify the inflammatory cascade involved revealed an upregulation of pro-inflammatory cytokines [9]. The first genome-wide gene-expression survey of BA-mice at different stages of bile duct obstruction was published recently [10]. Bezerra and colleagues compared the gene expression profiles in the extrahepatic bile duct tissue of Balb/c-mice with BA and healthy control animals. In contrast, we focused on the different gene expression in the liver of mice subjected to the same model, but compared infected mice that show the phenotype of BA versus infected mice without symptoms, thus trying to elucidate genes that are not related to the viral origin of this experimental model, but to the specific pathogenesis of BA.

Comparing the published results of Bezerra and the differences observed in this study, we found similarities in the up-regulation of genes involved in the Th1 pathway, such as CXCL9 and CXCL10, and in apoptosis: granzyme A and B, suggesting that these genes are not only involved in the reaction to the viral defence, but are also important for the development of the phenotype of BA. CXCL10 is a chemokine that targets T-cells and natural killer cells and is deemed to be a general marker of hepatic inflammation playing a role in tissue repair and regeneration [18]. Furthermore, it was reported that complement cascade members in concert with natural antibodies may participate in regulatory T-cell immunity [15]. Bezerra and colleagues describe many members of the complement cascade in their analyses, suggesting a modulating effect on bile duct inflammation and atresia. In agreement with such an observation, we also found activation of one complement factor (Perforin). However, in contrast to Bezerra and co-workers, we failed to find up-regulation of IFN gamma and TNF α in the liver of mice with BA using our comparative microarray approach. This may suggest that these cytokines are not critical for the development of the phenotype of BA in mice, but could also be explained by different comparison groups or time points of analysis. However, this was solely due to our analytical approach, which required coefficients of variation of 30% and less in order to be considered acceptable (see Materials and methods). The value of IFN gamma (foldchange 3.77; coefficient of variation 46%) and TNF α (fold-change 1.87; coefficient of variation 80%) were higher and, therefore, not included in further analysis. Other upregulated genes described in the previous publication were not included on our microarray and a comparision is therefore not possible.

Interestingly, very low expression of TIMD2 was observed in BA-positive mice. TIMD2 plays a critical role in the regulation of the Th2-type response with inhibition of IFN gamma [17]. Of potential importance: we could detect a down-regulation of IGF1 and GHR in mice with BA in agreement with a previous report on children with BA, in which low level of IGF1 was a characteristic finding [19]. Furthermore, it was speculated that obstructive cholestasis may lead to down-regulation of GHR and IGF1 expression [20].

In summary, our present study provides a basis for hypothesis generation and future experiments with the potential use of knockout mice that may enhance our understanding of the pathogenesis of BA and hopefully open up new avenues for therpeutic options in biliary atresia.

Acknowledgements The authors would like to thank Ms Birgit Teichmann for technical assistance and Ms Clare Boerner for revising the text. This work was supported by a grant (HiLFI) from the Hannover Medical School, Germany.

References

1. Petersen C (2005) Pathogenesis and treatment opportunities for biliary atresia. Clin Liver Dis (in press)
2. Schreiber RA, Kleinman RE (2002) Biliary atresia. J Pediatr Gastroenterol Nutr 35:11–16
3. Mack CL, Tucker RM, Sokol RJ, Karrer FM, Kotzin BL, Whitington PF, Miller SD.(2004) Biliary atresia is associated with CD4+ Th1 cell-mediated portal tract inflammation. Pediatr Res. 56:79–87
4. Riepenhoff-Talty M, Schaekel K, Clark H, Mueller W, Uhnoo I, Rossi T, Fisher J, Ogra PL (1993) Group A rotaviruses produce extrahepatic biliary obstruction in orally inoculated newborn mice. Pediatr Res 33:394–399
5. Petersen C, Biermanns D, Kuske M, Schakel K, Meyer-Junghanel L, Mildenberger H (1997) New aspects in a murine model for extrahepatic biliary atresia. J Pediatr Surg 32:1190–1195
6. Czech-Schmidt G, Verhagen W, Szavay P, Leonhardt J, Petersen C (2001) Immunological gap in the infectious animal model for biliary atresia. J Surg Res 101:62–67
7. Chan R, Tan CL, Czech-Schmidt G, Petersen C (2005) Computerized three-dimensional study of a rotavirus model of biliary atresia: comparison with human biliary atresia. Pediatr Surg Int 21:615–620
8. Shivakumar P, Campbell KM, Sabla GE, Miethke A, Tiao G, McNeal MM, Ward RL, Bezerra JA (2004) Obstruction of extrahepatic bile ducts by lymphocytes is regulated by IFN-gamma in experimental biliary atresia. J Clin Invest 114(3):322–329
9. Bezerra JA, Tiao G, Ryckman FC, Alonso M, Sabla GE, Shneider B, Sokol RJ, Aronow BJ (2002) Genetic induction of proinflammatory immunity in children with biliary atresia. Lancet 360:1653–1659
10. Carvalho E, Liu C, Shivakumar P, Sabla G, Aronow B, Bezerra J (2005) Analysis of the biliary transcriptome in experimental biliary atresia. Gastroenterol 129:713–17
11. Bosio A, Knorr C, Janssen U, Gebel S, Haussmann HJ, Muller T (2002) Kinetics of gene expression profiling in Swiss 3T3 cells exposed to aqueous extracts of cigarette smoke. Carcinogenesis 23:741–748
12. Cario G, Stanulla M, Fine BM, Teuffel O, Neuhoff NV, Schrauder A, Flohr T, Schafer BW, Bartram CR, Welte K, Schlegelberger B, Schrappe M. (2005). Distinct gene expression profiles determine molecular treatment response in childhood acute lymphoblastic leukemia. Blood 105:821–826
13. Petersen C, Grasshoff S, Luciano L (1998) Diverse morphology of biliary atresia in an animal model. J Hepatol. 28:603–607
14. Mack CL, Tucker RM, Sokol RJ, Kotzin BL (2005) Armed CD4+ Th1 effector cells and activated macrophages participate in bile duct injury in murine biliary atresia. Clin Immunol. 115(2):200–209
15. Carroll M (2004) The complement system in regulation of adaptive immunity. Nature Immunology 5:981–986
16. Ajuebor MN, Hogaboam CM, Proudfoot AI, Swain MG (2004) CCL3/MIP-1α is proinflammatory in murine T cell-mediated hepatitis by recruiting CCR1-expressing $CD4^+$ T cells to the liver. Eur J Immunol 34:2907–2918
17. Chakravarti S, Sabatos CA, Xiao S, Illes Z, Cha EK, Sobel RA, Zheng X, Strom T, Kuchroo V (2005) Tim-2 regulates T helper type 2 responses and autoimmunity. J Ex Med 202:437–444
18. Koniaris LG, Zimmers-Koniaris T, Hsiao EC, Chavin K, Sitzmann JV, Farber JM (2001) Cytokine-responsive gene-2/IFN-inducible protein-10 expression in multiple models of liver and bile duct injury suggests a role in tissue regeneration. J Immunol 167:399–406
19. Yoshida S, Nio M, Hayashi Y, Ohi R, Kawamura I, Goto T (2003) Serum insulinlike growth factor-1 in biliary atresia. J Ped Surg 38: 211–215
20. Held MA, Cosme-Blanco W, Difedele LM, Bonkowski EL, Menon RK, Denson LA (2004) Alterations in growth hormone receptor abundance regulate growth hormone signaling in murine obstructive cholestasis. Am J Physiol Gastrointest Liver Physiol 288:986–993